ARTICLE
Journal of Cellular Biochemistry 116:1222–1231 (2015)

Journal of Cellular Biochemistry

Internalization of Near-Infrared Fluorescently Labeled Activatable Cell-Penetrating Peptide and of Proteins Into Human Fibrosarcoma Cell Line HT-1080

Felista Tansi,[1] Eric Kallweit,[1,2] Christoph Kaether,[3] Katarina Kappe,[4] Christina Schumann,[2] Ingrid Hilger,[1] and Siegmund Reissmann[4,5]*

[1]*Institute of Diagnostic and Interventional Radiology, Department of Experimental Radiology, Jena University Hospital, Friedrich-Schiller University, Erlanger Allee 101, Jena 07747, Germany*

[2]*Ernst-Abbe-University of Applied Sciences, Carl-Zeiss-Promenade 2, Jena 07745, Germany*

[3]*Leibniz Institute for Age Research, Fritz-Lipmann-Institute, Beutenbergstr. 11, Jena 07745, Germany*

[4]*Jena Bioscience GmbH, Loebstedter Str. 80, Jena 07749, Germany*

[5]*Centrum of Molecular Biomedicine, Institute of Biochemistry and Biophysics, Friedrich- Schiller-University, Dornburger Str. 25, Jena 07743, Germany*

ABSTRACT

The internalization of near-infrared fluorescently labeled cargos into living cells and tissues allows a highly sensitive detection without interference from skin, porphins or other fluorescent cell and tissue compounds. In this study, the uptake of labeled bovine serum albumin and an antibody, into fibrosarcoma (HT-1080) cells was triggered by the formation of non-covalent complexes with different cell-penetrating peptides; uptake efficiency and intracellular localization were determined. To improve selectivity of internalization into tumor cells, a fluorescent activatable cell-penetrating peptide (ACPP) was synthesized and functionally characterized. This 25-mer peptide was designed to be activatable by Matrix-Metallo-Proteases (MMPs). Its uptake selectivity was estimated using cells with different MMP activities. J. Cell. Biochem. 116: 1222–1231, 2015.

KEY WORDS: CELL-PENETRATING PEPTIDES; HIV-TAT (47-57); MPGalpha; MPGbeta; CAD-2; PROTEODUCIN; HISTONES; BOVINE SERUM ALBUMIN; ACTIVATION BY MATRIX-METALLO-PROTEASES; NEAR INFRARED FLUORESCENT LABELED CARGOS; FORMATION OF NON-COVALENT COMPLEXES BETWEEN CARGO AND CPP; CPP-DEPENDENT UPTAKE EFFICIENCY; SELECTIVITY OF INTERNALIZATION; INTRACELLULAR TRAFFICKING; HUMAN FIBROSARCOMA HT-1080 CELLS

Cell-penetrating peptides (CPPs) are used for the transport of different cargos into cells, tissues, and organs. Peptides, proteins, nucleic acids, drugs, and nanoparticles can be internalized as cargos into live cells. CPPs can be either conjugated to the cargo or form non-covalent complexes. Because their uptake mechanism primarily requires binding to proteoglycans or ubiquitously occurring receptors [Snyder et al., 2005; Letoha et al., 2010; Ezzat et al., 2012] the *first generation of CPPs* had only a low cell- and tissue-selectivity. To overcome this drawback, several strategies have been developed. Most selective internalization helpers are hormone analogues such as ligands for G-protein coupled receptors, as well as ligands for the more widely distributed integrine-, chemokine-, and scavenger-receptors or syndecans and neuropilins.

Cancer and inflamed tissue are characterized by a low pH-value and hypoxia, recognized as hallmarks of a tumor. Additionally, cancer cells express matrix-metallo-proteases (MMPs). All these properties can be exploited to develop CPPs which internalize specifically into these cells or tissues. Thus, certain CPPs (pHLIPs) form the right uptake conformation only at low pH-values [Reshetnyak et al., 2008; Andreev et al., 2010; Musial-Siwek et al., 2010a, b; Diao et al., 2011].

Activatable CPPs are the most recent and sophisticated development. Activation occurs on the target tissue based on its specific

Conflict of interest: None.

*Correspondence to: Prof. Siegmund Reissmann, Institute of Biochemistry and Biophysics, Friedrich-Schiller-University, Dornburger Str. 25, Jena 07743, Germany.
E-mail: siegmund.reissmann@uni-jena.de

Manuscript Received: 8 September 2014; Manuscript Accepted: 19 December 2014
Accepted manuscript online in Wiley Online Library (wileyonlinelibrary.com): 25 December 2014
DOI 10.1002/jcb.25075 • © 2014 Wiley Periodicals, Inc.

biochemical properties. An excellent innovation is the development of a protease activatable CPP by the group of Roger Tsien [Aguilera et al., 2009; Olson et al., 2009,2010]. Membrane-bound and secreted proteases of tumor cells, mostly secreted matrix-metallo-proteases (MMPs) [van Duijnhoven et al., 2011], as well as plasmin, elastase [Whitney et al., 2013] and proteases in inflamed tissue, activate these CPPs. Activation occurs by proteolytic cleavage of a designed and sensitive linker between a positively charged CPP and a negatively charged capping peptide sequence. After activation, the released peptide fragment is capable of transporting cargos into specific target cells, primarily tumor, and metastasizing cells. The peptide can target cells with fluorescent or other markers which enable their detection [Nguyen et al., 2010; Olson et al., 2012; Savanier et al., 2013].

In this study, we describe the CPP-dependent uptake efficiency and intracellular trafficking of near-infrared fluorescent cargos (BSA, monoclonal Ab) into human fibrosarcoma HT-1080 cells. Furthermore, we report on the uptake of a near-infrared fluorescently labeled activated sequence from the ACPP into cancer cell lines. HT-1080 cells express the MMPs 2 and 9. The linker of the ACPP was designed for cleavage by these proteases.

In many cases, *ACPPs* are *covalently bound to dendrimers* such as poly (amidoamine) dendrimers [Nguyen et al., 2010] or to the surface of nanoparticles, which can contain more than one label and more than one cargo [Olson et al., 2010]. Nanoparticles and biopolymers accumulate passively in tumors because solid tumors commonly have a more permeable structure, impaired lymphatic drainage, and sloppy tumor vasculature with poorly aligned endothelial cells.

Olson and co-workers described the successful detection of tumor cells with an ACPP, which was labeled with a fluorescence marker at a cysteine residue, added to the C-terminus of the CPP [Olson et al., 2012]. In our case we inserted the Cys-residue into the linker at the N-terminus of the CPP. Thus, the neighborhood of the fluorescence marker can influence the cleavage site.

Because acquisition of *near-infrared fluorescence* (NIRF) is not disturbed by porphyrins or other fluorescent cell- and tissue-compounds the fluorescent label can be detected in the intact animal. Thus, NIRF-measurements are very sensitive and allow the macroscopic detection of very small tumors and metastases with a diameter of below 200 μm. As such, labels as well as chemically synthesized compounds and infrared fluorescent proteins [Shu et al., 2009] can be used.

To some degree, chemical properties such as hydrophobicity and hydrophilicity of the chosen fluorescent dyes can influence uptake into tissues and organs. Thus, Hamann et al. (2011) found an uptake-selectivity for infrared fluorescent dyes alone. Depending on the number of negatively charged sulfonate groups, the dyes bind with different affinities to plasma proteins leading to different biodistribution and excretion pathways in animal experiments. But, in our case properties of BSA, antibody and ACPP were more important for uptake and distribution than the fluorescent markers used.

Fluorescent ACPPs allow a marking of the margin between normal and cancer tissue, which grants a more accurate and complete surgical resection of cancer tissue. To some degree this method is comparable to the use of *5-aminolevulinic acid* in surgery [Colditz and Jeffree, 2012], mainly in neurosurgery [Cornelius et al., 2014; De la Garza-Ramos et al., 2014; Puppa et al., 2014]. The 5-amino-levulinic acid, owing to the high metabolic activity in cancer cells, is converted into the fluorescent molecule protoporphyrin IX which can be used for fluorescence-guided tumor resection.

Though both methods are suitable for application in cancer surgery, their tumor selectivity, the fluorescence yield and ability to invade, can vary. In our opinion ACPPs with highly effective near-infrared fluorescent labels are superior to the application of 5-amino-levulinic acid, in particular for slowly growing carcinomas or for those which are located deep within organs.

MATERIALS AND METHODS

CELL-PENETRATING PEPTIDES

Cell-penetrating peptides MPGα, MPGβ, CAD-2, HIV-TAT(47–57), and the cocktail JBS-Proteoducin were obtained from Jena Bioscience (Jena, Germany), Histone type II-AS (Calf thymus) was obtained from Sigma-Aldrich (Taufkirchen, Germany).

MPGα: Ac-GALFLAAALSLMGLWSQPKKKRKV-NH_2-CH_2-CH_2-SH [Chaloin et al., 1997; Deshayes et al., 2004]

MPGβ: Ac-GALFLGFLGAAGSTMGAWSQPKKKRKV-NH_2-CH_2-CH_2-SH [Chaloin et al., 1997; Deshayes et al., 2004]

CAD-2: GLWRALWRLLRSLWRLLWKA-NH_2-CH_2-CH_2-SH (desacetyl Lys^{19}-CADY) [according to CADY: Crombez et al., 2009; Kurzawa et al., 2010]

HIV-TAT(47–57): YGRKKRRQRRR [Vives et al., 1997; Ignatovich et al., 2003]

JBS-Proteoducin: Cocktail of different cell-penetrating compounds.

CARGO PROTEINS

BSA that was covalently coupled to the near-infrared fluorescent dye DY-676 (BSA-DY676) was purchased from Jena Bioscience (Jena, Germany). The humanized anti-HER2 monoclonal antibody, Trastuzumab was obtained from Hoffmann La-Roche AG (Grenzach-Wyhlen, Germany) and covalently conjugated to the near-infrared fluorescent dye, DY652 (DYOMICS GmbH, Jena, Germany).

SYNTHESIS OF ACPP (EEEEEEEEE-APLGAGC-RRRRRRRRR-NH_2)

ASSEMBLY OF PEPTIDE

The linear 25-mer peptide was synthesized by the solid phase method on Tentagel-Amide resin (loading 0.23 mmol/g resin) using the automated instrument ResPep SL (Intavis, Bioanalytical Instruments AG, Cologne, Germany). Resin, protected amino acid derivatives and coupling reagent were also purchased from Intavis, if not otherwise indicated. The following amino acid derivatives were used for coupling: Fmoc-Arg(Pbf)-OH (Iris Biotech GmbH, Marktredwitz, Germany), Fmoc-Cys(Trt)-OH, Fmoc-Gly, Fmoc-Ala, Fmoc-Leu, Fmoc-Pro (all Intavis), Fmoc-Glu(OBu^t)-OH (Iris Biotech GmbH). Abbreviations, acronyms and symbols for amino acids, protecting groups, and reagents were used according to Journal of Peptide Science 2006, 12:1–12.

Coupling was performed with five equivalents of amino acid derivatives and five equivalents PyBOP (benzotriazol-1-yloxytripyrrolidinophosphonium hexafluorophosphate, Merck Schuchardt OHG, Hohenbrunn, Germany) for the 13 C-terminal amino acids and with TBTU (N-[(1H-benzotriazol-1-yl)(dimethylamino) methylene]-N-methyl-methanaminium tetrafluoroborate N-oxide, Merck Schuchardt) for all other N-terminal amino acids. NMM (N-methylmorpholine, Merck Schuchardt) was used as the base. Each coupling was repeated twice with a coupling time of 20, 30, to 40 min each, depending on the length of the growing peptide chain. For developing an optimized strategy certain crucial steps were checked by HPLC and ESI-MS. After each final coupling the remaining free amino groups were capped with acetanhydride. Removal of the Fmoc-group was performed with 20% piperidine (Sigma-Aldrich GmbH, Taufkirchen, Germany) in DMF (Merck KGaA, Darmstadt, Germany) in two steps between 10, 15, and 20 min increasing with the length of the peptide chain.

The free peptide was obtained by the double cleavage from the resin and simultaneously removing the Boc-, Trt- and OBut-groups with 95% TFA (trifluoro acetic acid, Merck KGaA), 2.5% TIS (triisopropylsilane, Merck KGaA), and 2.5% H_2O for 2 h each. Yield calculated from resin loading with protected precursor: 60%. After concentrating the TFA-cocktail in vacuo to 1 ml, followed by precipitation with tert.-butyl-methylether and separation by centrifugation, the pellets were thoroughly washed with tert.-butyl-methylether, dissolved in aqueous tert. butanol (80%), filtrated through glass wool, lyophilized, and purified twice by semi-preparative HPLC as described below. The 25-mer peptide was homogeneous by HPLC and showed well developed MS spectra. MW(calculated) = 3154.9 Da, MW(found) = 3154.07 Da.

SEMIPREPARATIVE REVERSED-PHASE HPLC

The crude peptide was purified by semipreparative HPLC on JASCO chromatograph PU-2087 Plus equipped with a column YMC Pack ODS (250 × 30 mm, 10 μm particle size, YMC GmbH, Dinslaken, Germany) and using a gradient of 5%–65% B in 120 min. A was 0.1% TFA in water and B was 0.1% TFA in acetonitrile. The flow rate was 20.0 ml/min. Detection was accomplished at 220 nm.

ANALYTICAL REVERSED-PHASE HPLC

Analytical HPLC was performed on JASCO chromatograph PU-2080 Plus (JASCO, Labor- und Datentechnik GmbH, Gross-Umstadt, Germany) with an AppliCHROM column OTU LipoMare (250 × 4.6 mm, C18, 5 μm particle size). For elution a gradient was used 10%–70% B in 120 min. A was 0.1% TFA in water and B 0.1% TFA in acetonitrile. The flow rate was 1.0 ml/min. Detection was accomplished at 220 nm (JASCO, UV-2075 Plus).

SYNTHESIS OF EEEEEEEEE-APLGAGC-(SUCCINIMIDE-DY676)-RRRRRRRRR-NH_2 THROUGH LABELING OF 25-MER ACPP WITH THE NEAR-INFRARED FLUORESCENCE MARKER DY676

Two-hundred micrograms (0.05 μMol) trifluoroacetate of the 25-mer peptide, purified by HPLC, were dissolved in 20 μL 1 M Tris-buffer, pH 7.2 and carefully vortexed with 1 μL Tris-(2-carboxyethyl) phosphine hydrochloride (TCEP), dissolved in ultra-pure water according to instructions for the "Atto 488 Protein Labeling Kit" (Jena Bioscience, Jena, Germany). Coupling of 200 μg (0.21 μMol) DY676-Maleimide (Dyomics, Jena, Germany) was performed according to the instructions of the Jena Bioscience Kit with the following modifications: Atto-488-Maleimide was replaced by DY676-Maleimide, the excess of fluorescent label reduced to a ratio of fourfold over peptide. Moreover, no glutathione (GSH) was added and after running the reaction for 2 h, the mixture was immediately lyophilized. Purification of crude reaction product was performed by analytical high performance liquid chromatography (HPLC) on JASCO chromatograph PU-2080 Plus with a C18 column OTU LipoMare (220 × 4.6 mm, 5 μm). For elution a gradient was used 10%–30% B for 40 min and 30%–50% for 20 min. A was 0.1% TFA in water and B 0.1% TFA in acetonitrile, using a flow rate of 1.0 ml/min and accomplishing detection at 220 nm.

Fluorescent ACPP was eluted at a higher acetonitrile concentration than free ACPP, and unreacted ACPP could therefore be recovered. Both the fluorescent marker and its hydrolysed products were eluted at higher acetonitrile concentrations than the labeled ACPP. A representative HPLC-elution profile is shown in Figure 3.

MALDI-TOF MASS SPECTROMETRY

All peptides and fractions are characterized by MALDI-mass spectrometry. MALDI-TOF mass spectra were measured on Ultraflextreme (Brucker Daltonics, Leipzig, Germany). Detection occurs in region m/z 700–6000. Peptide 2 Calibration Standard (Brucker Daltonics) was used as standard, containing nine peptides with increasing molecular weights from bradykinin 1–7 up to somatostatin 28. The determined molecular mass of 3154 Da corresponds to unlabeled ACPP and 4062 Da to DY676-labeled 25-mer ACPP.

CELL LINES

The human fibrosarcoma cell line, HT-1080 (Cell Lines Services, Heidelberg, Germany) was cultivated in RPMI medium (Gibco®, Life Technologies GmbH, Germany) supplemented with 5% (v/v) fetal calf serum (FCS). The immortalized human microvascular endothelial cells (HMEC-1) were got from Centers for Disease Control and Prevention, USA, and cultured in MCDB 131 medium (Gibco®) supplemented with 10% (v/v) FCS, 1% (v/v) GlutaMAX™ (Gibco®), 1 μg/ml hydrocholesterol (Sigma-Aldrich, Taufkirchen, Germany), 10 ng/ml epidermal growth factor (Gibco®). The human breast adenocarcinoma cell lines, BT-474, and MDA-MB231 were purchased from the Cell line service (CLS, Germany) and cultured in DMEM/Ham's F12 medium containing 10% (v/v) FCS (Gibco®). All the cell lines were cultured at standard conditions (37°C with 5% CO_2 and 95% humidity).

PREPARATION OF CPP STOCK SOLUTIONS

All CPP samples (0.5 mg each) were dissolved in 1.25 ml of sterile Argon-degassed water according to the manufacture's instructions

(Jena Bioscience). Briefly, the solution was thoroughly mixed by vortexing, quickly frozen in liquid nitrogen and thawed (5 cycles), then sonicated for 5 min. The resulting stock solutions were either used immediately or stored in aliquots at −20°C.

PREPARATION OF CPP-PROTEIN COMPLEXES

The non-covalent CPP-protein complexes were prepared as reported earlier [Mussbach et al., 2011]. Briefly, 14.7 pMol of the cargo protein BSA-DY676, (BSA coupled to the near-infrared fluorescent dye, DY676) or 10 pMol Trastuzumab-DY-652 and a 10 molar excess of the respective CPP stock solutions were dissolved in 100 μl of Hank′s buffered saline solution (HBSS, pH 7.4 from PAA, Pasching Austria), respectively. Thereafter, the solutions were mixed carefully by a pipetting step repeated six times, then incubated for 30 min at 37°C to allow complex formation to take place.

CPP-BASED INTERNALIZATION OF BSA-DY676 AND TRASTUZUMAB-DY652 INTO HUMAN FIBROSARCOMA CELLS HT-1080

For qualitative analysis by confocal microscopy, 30,000 cells (HT-1080) or 50,000 cells (BT-474) were grown on poly-L-lysine-coated 8-well culture slides (BD Biosciences, Heidelberg, Germany) for 16 h. While complex formation was running, the cells were prepared for internalization as reported earlier [Mussbach et al., 2011]. Briefly, the culture medium was aspirated and the cells were washed three times with HBSS. The preformed complex solution (200 μl) was added to the cells then quickly diluted by adding 300 μl of serum free medium containing 1.5% DMSO (v/v), 1 mM Aprotinin (Trasylol, Schering AG, Germany) and 0.5 mM EDTA (Sigma-Aldrich). The chamber slides were incubated for 2 h at 37°C in a 95% humidified atmosphere with 5% CO_2. Thereafter, 400 μl of the medium were removed and replaced by complete growth medium. The cells were further cultured for approximately 22 h under standard culture conditions.

In order to estimate and quantify the level of internalization induced by different CPPs, 2.10^6 cells were grown for 16 h in 25 cm^3 tissue culture flasks in 5 ml complete medium. The cells were washed and prepared for internalization tests similar to those on culture slides as described above. The concentrations used remained the same, except 1.5 ml serum-free medium was added to the cells after addition of the complex and 5 ml complete medium added after 2 h pre-incubation of the cells with the complex. To control whether the Trastuzumab-was still active and would bind the HER2/neu protein on cells, the breast cancer cell line BT-474, which is characterized by a high expression of HER2 was used. Preparation of the cells was similar to the HT-1080 cells.

For internalization the 25-mer near-infrared fluorescence (NIRF)-labeled ACPP-DY676 was dissolved in HBSS at a concentration 0.25 μg/test, added to washed cells and quickly diluted with 300 μl of serum-free medium containing DMSO, Aprotinin, and EDTA in the same concentrations as described above for internalization of CPP-protein complexes. Furthermore, different cell lines used were prepared similar to the HT-1080 cells, and grown in their corresponding growth media. The free dye DY676 was used as a control at a concentration of 0.2 μg/test.

QUALITATIVE ANALYSIS OF INTERNALIZATION BY CONFOCAL MICROSCOPY

The treated cells were washed once with HBSS, twice with 10 mM glycine buffer, pH 3 (Jena Bioscience GmbH), then once again with HBSS and fixed for 1 h at RT with 3.7% (v/v) formaldehyde in HBSS. Following two washing steps, the chambers were separated and the cells mounted with PermaFluor (Thermo Fisher Scientific GmbH, Schwerte, Germany) containing the DNA stain Hoechst-33258 (Applichem GmbH, Darmstadt, Germany), then covered with glass cover-slips and air dried for 1 h at room temperature in the dark. The cells were subsequently imaged on the LSM510-META confocal microscope (Zeiss, Jena, Germany). The nuclei were visualized with a 405 nm laser diode and a 420–480 nm band pass filter, whereas the near-infrared fluorescent dyes DY-676 and DY652 were excited with a 633 nm Argon laser and emission detected with a 650 nm long pass filter. For visualizing the Golgi apparatus, cells were processed for immunofluorescence according to Krämer et al. (2013); with an Alexa-488-antibody against GM130 (Giantin, mAb G1/133, obtained from Enzo Life Sciences, Germany), an early *cis* Golgi marker.

NEAR-INFRARED FLUORESCENCE IMAGING AND SEMI-QUANTITATIVE ANALYSIS OF INTERNALIZATION

The transduced cells in tissue culture flasks were also washed once with 2 ml HBSS, twice with 2 ml of 10 mM glycine, pH 3, then once with 2 ml HBSS. Finally, the cells were scraped in 2 ml HBSS and pelleted by centrifugation (1000*g*) in 15 ml falcon tubes. The supernatant was removed then the cells re-suspended in 500 μl HBSS, transferred to 500 μl Eppendorf tubes and further pelleted. The cell pellets in the Eppendorf tubes were imaged using the Maestro in vivo fluorescence imaging system (Maestro™, CRi, Woburn, UK) by exciting the near-infrared dye, DY676 with filters for the excitation range 615–665 nm and emission was acquired with a cut-in filter (>700 nm). Evaluation and extraction of background auto-fluorescence of untreated cells was performed with the Maestro-software according to the manufacturer′s instructions. Semi-quantitative analysis of the fluorescence intensities of cell pellets was performed by assigning a region of interest (ROI) to each pellet (target) and another on the tube region with HBSS alone. Fluorescence intensities were deduced as an average signal (scaled counts/s). This represents count levels after scaling for exposure time, camera gain, binning and bit depth, and makes the measurements comparable to each other.

STATISTICAL ANALYSIS

Data are expressed as means ± standard deviation. Except otherwise indicated, statistical significance was determined by a one way ANOVA analysis using SigmaPlot 12.0. A *P*-value less than or equal to 0.05 was considered as statistically significant.

RESULTS AND DISCUSSION

In order to test the transport efficiency of different CPPS, which have been already used for formation of non-covalent complexes, a near-infrared fluorescent labeled BSA and the clinically approved humanized monoclonal antibody to human epidermal growth factor receptor 2 (HER2) were used as cargos. The main aim was to study the feasibility of CPP-based imaging of tumor cells, the selectivity of various CPPs and the influence of the cargo on the internalization method. We present results of CPP-based delivery of cargo proteins into the human fibrosarcoma cell line HT-1080 for near-infrared imaging purposes. Furthermore, we present synthesis, labeling, and uptake of a protease activatable CPP.

TRANSPORT EFFICIENCY OF DIFFERENT CPPS FOR NIR-FLUORESCENT PROTEINS INTO HUMAN FIBROSARCOMA HT-1080 CELLS

The different CPPs revealed distinct abilities to internalize BSA and the humanized antibody Trastuzumab. Near-infrared fluorescence imaging provided characteristic fluorescence of the internalized BSA-DY676 in cell pellets (Fig. 1, part A, fluorescence images of

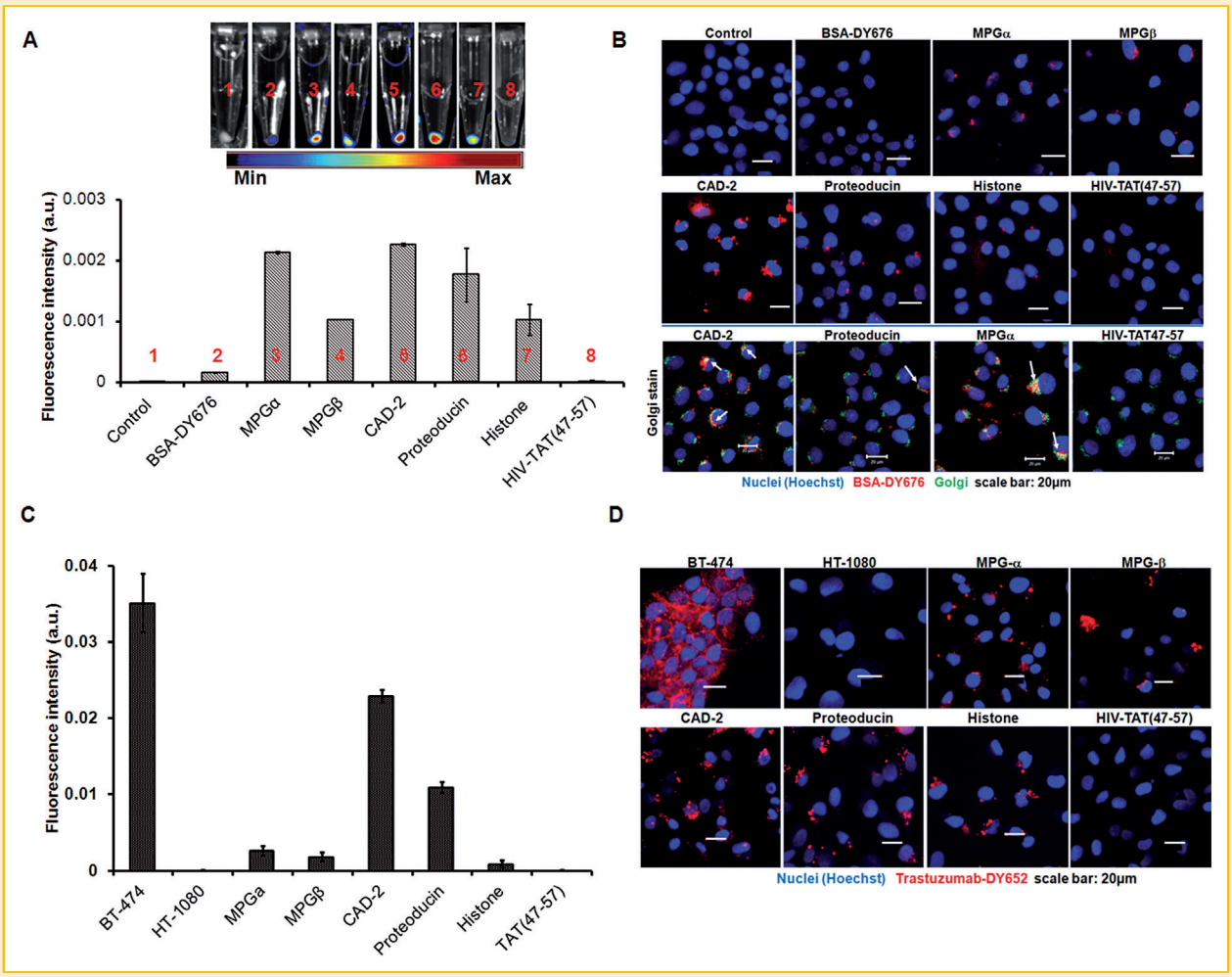

Fig. 1. CPP-based internalization of BSA-DY676 and Trastuzumab-DY652 into the fibrosarcoma cell line HT-1080. (A) NIRF imaging and semi-quantitative analysis reveal the highest fluorescence of internalized BSA-DY676 when complexed with MPGα, CAD-2 or JBS-Proteoducin, whereas lower rates are achieved with MPGβ and Histone and no transport is seen with HIV-TAT(47–57). a.u.: arbitrary units. Each bar represents the mean of $n = 3 \pm$ S.D. $P > 0.05$ (no significance) for CAD-2 versus MPGα, versus JBS-Proteoducin. $P = 0.001$ (significant) for the internalization of BSA-DY676 with CAD-2, MPGα, and JBS-Proteoducin versus Histone and MPGβ. $P > 0.05$ (no significance) for Histone versus MPGβ. $P \leq 0.01$ (significant) all CPPs versus HIV-TAT(47-57). (B) Confocal microscopic images of cells after internalization of BSA-DY676. The transported BSA-DY676 co-localizes with the Golgi (white arrows). (C) NIRF imaging and semi-quantitative analysis reveal the highest fluorescence of internalized Trastuzumab-DY652 when complexed with CAD-2 or JBS-Proteoducin, whereas lower rates are achieved with MPGα, MPGβ, and Histone. No transport is seen with HIV-TAT(47–57). a.u.: arbitrary units. Each bar represents the mean of $n = 3 \pm$ S.D. $P < 0.001$ for internalization via CAD-2 versus JBS-Proteoducin. $P \leq 0.001$ for CAD-2 or JBS-Proteoducin versus MPGα, MPGβ, and Histone. $P > 0.05$ (no significance) for the CPPs MPGα versus MPGβ versus Histone. (D) The internalized antibody is partially localized in the cis-Golgi, similar to the BSA-DY676, with some minor fluorescence localized in vesicles. BT-474 cells express HER2 and serve as a positive control for the receptor affinity of Trastuzumab, whereas HT-1080 lacks HER2 receptor expression hence no signal.

tubes). Semi-quantitative analysis of the fluorescence intensities showed some differences. Whereas complex formation with MPGα, CAD-2 and Proteoducin resulted in high internalization levels, hence high fluorescence intensities, MPGβ and histone were only able to internalize relatively lower levels of the BSA-DY676 (Fig. 1, part A, bar diagram). Free BSA-DY676 was not taken up by the HT-1080 cells. Furthermore, it can be seen that the HIV-TAT(47–57) was unable to internalize cargo proteins into these cancer cells.

According to [Keller et al., 2013] the efficiency of uptake depends mainly on the cell type, CPP, and on the particular cargo. Despite the low cell- and tissue-selectivity of CPPs of the first generation, certain differences can be observed. These differences can be ascribed to the lipid composition of the cell membrane and on the abundance of cell surface proteoglycans such as syndecans, and receptors such as CXCR4- and scavenger- receptors. In this work, non-covalent complexes of labeled BSA and Trastuzumab with different CPPs were formed. Formation and stability of the complexes depend on ionic, hydrophobic, and polar interactions, H-bonds as well as on the conformation and flexibility of the CPP and the both cargos. Compared to reports on other cell lines such as HeLa, COS-7, NIH 3T3, Jurkat, NB-4, Kasumi-1, and *Leishmania tarentolae* cells, the rank orders of CPPs for BSA internalization were to some degree different [Mussbach et al., 2011; Keller et al., 2013]. Whereas JBS-Proteoducin, MPGβ and MPGα had the highest transport efficiency in the above mentioned cell lines, the present work reveals that for the HT-1080 cells the uptake efficiency of complexes with MPGβ was significantly lower. Some differences were also seen with Trastuzumab as the cargo protein, whereby only low levels were internalized when complexed with MPGα and MPGβ and very high levels were internalized when complexed with CAD-2 and JBS-Proteoducin (Fig. 1, parts C and D). For the cargo BSA-DY676 the CAD-2 showed a significantly higher efficiency ($P < 0.001$) than all the other CPPs studied. MPGα and JBS-Proteoducin showed no significant difference. However, both MPGα and JBS-Proteoducin revealed significantly higher ($P < 0.001$) abilities to internalize BSA-DY676 than MPGβ, Histone, and HIV-TAT(47–57). Furthermore, no significant difference ($P > 0.05$) was seen for Histone versus MPGβ, whereas all the CPPs revealed a significantly higher internalization of BSA-DY676 ($P < 0.001$) than the HIV-TAT(47–57). For the cargo Trastuzumab-DY652, internalization via CAD-2 was higher than with JBS-Proteoducin ($P < 0.001$), whereas CAD-2 and JBS-Proteoducin internalize significantly higher levels of Trastuzumab ($P < 0.001$) than MPGα, MPGβ or Histone. Furthermore, there is no significant difference ($P > 0.05$) for the internalization of Trastuzumab by MPGα, MPGβ or Histone. The strongly positively charged peptide HIV-TAT(47–57) was unable to transport BSA or Trastuzumab, possibly because of a failure to form stable complexes with the cargo proteins. Estimated differences in rank orders indicate the influence of different factors on a complex process with the steps: complex formation, binding to cell surface, and internalization.

However, the internalization of strongly positively charged peptides is well documented for covalently coupled cargos such as the internalization of proteolytic activated ACPPs with covalently coupled markers or drugs and the uptake of HIV-TAT(47–57) with covalently linked nanoparticles [Torchilin, 2008]. In contrast to the inability of HIV-TAT(47–57) to form non-covalent complexes, the strongly positive charged active fragment resulting from the cleavage of the ACPP-DY676 penetrates the cells directly. Furthermore, the active fragment transports the NIRF-marker in a covalently bound form. This could be seen in the different fluorescence intensities of cancer cell lines treated with the protease activatable peptide (Fig. 2, parts A and B).

DETECTION OF NEAR-INFRARED FLUORESCENCE IN THE GOLGI APPARATUS

The intracellular localization pattern of the BSA-DY676 is the same, irrespective of the CPP used for internalization. To pinpoint the exact

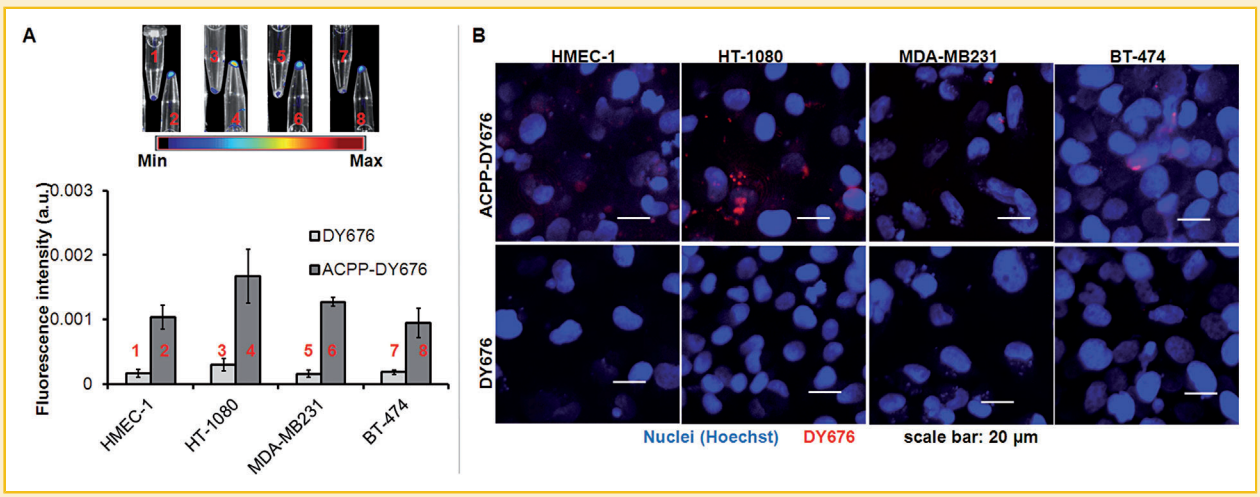

Fig. 2. Uptake of ACPP-DY676 into different cell lines. (A) NIRF imaging and semi quantitative analysis reveal the highest fluorescence of internalized ACPP DY676 (0.25 µg/test) in the fibrosarcoma cell line HT-1080. The free dye DY676 was used as a control at a concentration 0.2 gµ/test. Only negligible levels of the free DY676 are taken up by all the cell lines. a.u.: arbitrary units. Each bar represents the mean of n = 3 ± S.D. (B) Confocal microscopic images of cells after internalization of ACPP -DY676. The internalized ACPP-DY676 reveals minor fluorescence localized in vesicles.

localization of the cargo, the Golgi of cells treated with complexes formed from BSA-DY676 with CAD-2, Proteoducin, MPGα or HIV-TAT(47–57) were stained as described in the methods section. A partial co-localization of the internalized BSA-DY676 with the Golgi was evident, suggestive of Golgi/late endosomal localization. Co-localization can be seen as a yellow fluorescence of overlapping green (Golgi) and red (BSA-DY676) fluorescence, whereas residual green fluorescence of Golgi and vesicular red fluorescence of BSA-DY676, reveal areas with no co-localization (Fig. 1, part B). The Golgi apparatus was stained with a monoclonal antibody against the Golgi protein Giantin (GM130), the largest Golgi-membrane protein.

In our previous studies with the six cell lines mentioned above, we detected fluorescent cargos in cell vesicles, nuclei, cytoskeleton, and cytosol, as well as in the nucleus and kinetoplast of the protozoa *Leishmania tarentolae*, but never in the Golgi-apparatus. Other authors have found various CPP-cargo complexes localized in the nucleolus [Radis-Baptista et al., 2008], in mitochondria [Szeto et al., 2005; Yousif et al., 2009] and in lysosomes [Dekiwadia et al., 2012]. The intracellular trafficking depends on localization sequences of the individual CPPs or corresponding cargos and can be influenced by fluorescence labels [Szeto et al., 2005]. As commonly accepted, CPPs are internalized mainly by endocytic pathway and therefore can easily reach late endosomes or the Golgi. Both organelles are concentrated near the microtubule organizing centre and partially overlap at the resolution of light microscopy. The fluorescence of co-localized cargo with the Golgi can be seen predominantly in this area. Furthermore, several vesicles in close vicinity of the Golgi reveal fluorescence of the cargo alone, strengthening the fact that transport of the cargo follows the endocytic path through Golgi and endosomes. This is supported by the strong accumulation (vesicular fluorescence) of the BSA-DY676 in vesicles (Supplementary Figure S1) following CPP-based internalization into cells that were treated with chloroquine in a very low concentration (2 μM, instead of 120 μM as commonly used for release of cargo from endosomes). Chloroquine leads at these concentrations to swelling of the vesicles, which can be seen in this Supplementary Figure.

SYNTHESIS AND LABELING OF ACPP

The linker sequence of the ACPP was designed for activation by MMPs 2 and 9, explained in detail in "Activation of 25-mer ACPP by Matrix-Metallo-Proteases." Blockade of the positively charged penetrating nona-arginine was achieved with nine glutamic acid residues. For the coupling of the fluorescence label a cysteine residue was added to the C-terminus of the linker. The design resulted in a 25-mer peptide.

With careful analysis to optimize the coupling conditions, the nine C-terminal arginine residues and the linker sequence were assembled more smoothly than expected and with sufficient coupling rates; the following nine Glu-residues led to strong aggregation and reduced the coupling yields probably via hydrophobic interactions. The route and conditions of the synthesis are described in "Methods." The resulting crude product had a poor solubility. The occurrence of some failure sequences required a twofold purification by HPLC. Analytical characterization was performed by MALDI-TOF mass spectrometry.

LABELING OF ACPP

Coupling of the NIR-fluorescence marker was performed by attaching maleimide to the free SH-group of ACPP. To reduce disulfide bridges in the ACPP which can be formed via air oxidation, Tris-(2-carboxyethyl) phosphine hydrochloride (TCEP) was used. This reduction must be performed before adding the fluorescence label conjugated to maleimide. TCEP can however also reduce and inactivate the C-C double bond in the maleimide-moiety. We used a reduced level of the fluorescence marker than recommended and stopped the reaction by lyophilization without the addition of glutathione. This procedure allowed an improved separation of all components from the reaction product by HPLC and a recovery of unreacted ACPP. Figure 3 shows the HPLC elution diagram of DY676-ACPP together with the resulting molecular weights for the peaks. It was observed that the reaction was incomplete and that the maleimide-moiety was hydrolyzed to some degree. The fluorescent ACPP used in the following experiments was purified by analytical HPLC as described above.

ACTIVATION OF 25-MER ACPP AND INTERNALIZATION OF FLUORESCENT PARTIAL SEQUENCE

Many different subtypes of Matrix-Metallo-Proteases (MMPs) are known [Murphy and Nagase, 2008; Sbardella et al., 2012]. These Zn-proteases perform several physiological and pathophysiological functions. Tumors and their metastases express mainly MMPs of subtypes 2 (Gelatinase-A), 3 (Stromelysin-1), and 9 (Gelatinase-B). Owing to their enzymatic activity and their expression in neoplastic but not healthy tissue, they present good targets that can be used to address tumors for diagnosis and therapy. In our case the inactive fluorescent labeled ACPP should be activated by cleavage of the linker between negatively and positively charged parts of the 25-mer peptide. The amino acid sequence of this linker should be selectively and also easily cleavable by these MMPs.

The substrate specifity profile of MMPs is broad and the cleavage sites are overlapping [Murphy and Nagase, 2008; Sbardella et al., 2012]. In natural substrates with high molecular weights the scissile peptide bond is formed by 3-D-conformation [van Duijnhoven et al., 2011] and possibly more specifically than in low-molecular weight substrates or linkers. In the design of the linker sequence, sufficiently high cleavage selectivity as well as a good susceptibility to proteolytic cleavage is important. The application of ACPPs in diagnosis and therapy requires an intact peptide that can transport cargos into living cells, tissues, and organs selectively. However, other proteases can also cleave the linker and degrade the CPPs. For this reason CPPs with D-amino acids or other non-proteinogenic amino acids have also been used.

Although linker cleavage can be estimated with recombinant enzymes, experiments with living cells provide a more precise determination of the selectivity of internalization into cancer cells. In our study, in contrast to earlier ACPPs, the fluorescence marker is coupled to a cysteine residue in the linker sequence. Thus the

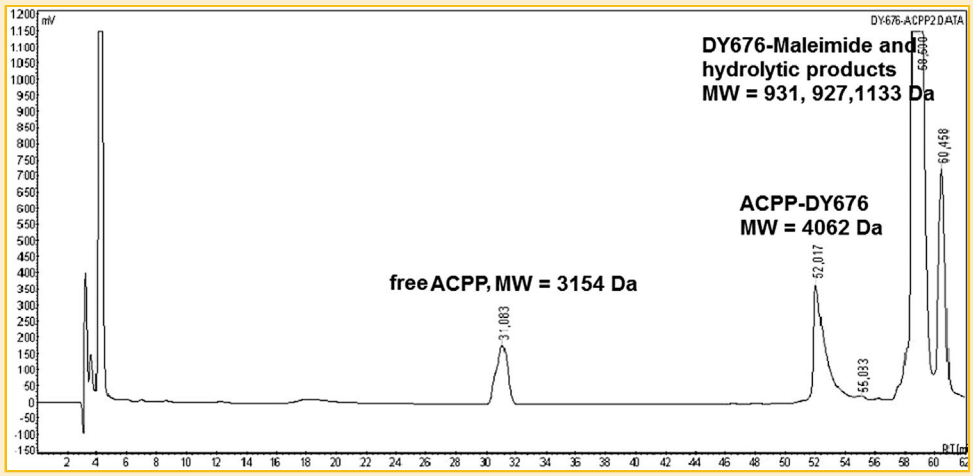

Fig. 3. Purification of ACPP-DY676 by HPLC and characterization of fractions by MALDI-MS. Covalent coupling of the fluorescent dye, DY-676 to the 25-mer peptide ACPP with one free SH-group was performed via maleimide. The lyophilized crude reaction product contains besides buffer, TCEP, unreacted ACPP, labeled ACPP, maleimide derivative of DY676 and hydrolyzed dye product. Molecular weights, determined by MALDI TOF measurements, allow assignment of each peak. Labeled ACPP can be isolated with very good purity and in a sufficient amount.

hydrophobic skeleton of the label DY676, with two hydrophilic sulfonic acid and one carboxylic acid residues is able to influence the interaction with the MMPs or change the preferred scissile bond. We expected a cleavage between residues Gly[13] and Ala[14]. Generally, MMPs cleave a peptide bond before a residue with a hydrophobic side chain [Murphy and Nagase, 2008] suggesting that a cleavage between Gly[15] and Cys(maleoimide-DY676)[16] would be possible, too. Ala[14] could be favored because of the neighborhood of Pro at position P3 from the scissile bond. With experiments using cancer cells, it is not possible to differentiate between these theoretical possibilities of cleavage. However, distinct activation and internalization of the labeled ACPP-fragment could be detected. We assume that the following sequence was internalized: AGC(SUCCINIMIDE-DY676)-RRRRRRRRR-NH_2.

The use of cell lines derived from different cancer types and stages revealed several differences in the level of activation and internalization of the ACPP. For example, the breast cancer cell line BT-474, which is characterized by a high level of the poor-prognosis tumor marker HER2/neu, revealed a lower level of ACPP-DY676-based fluorescence after 22 h incubation than the less aggressive HER2/neu negative breast cancer cell line MDA-MB231. The immortalized human microvascular endothelial cell line (HMEC-1), a non-cancer cell line, also revealed a comparably high level of ACPP-DY676-derived fluorescence. Compared to this, the human fibrosarcoma cell line HT-1080, which expresses MMPs 2 and 9, showed the highest fluorescence intensities of internalized ACPP-DY676. However, there was no statistical significance ($P = 0.057$) for internalization of ACPP-DY676 by the HT-1080 cells, compared to the other cell lines. Microscopic images revealed evidence that the ACPP-DY676, though at a low concentration, was visibly localized within the cells. In contrast to these observations, the free DY676 could not be taken up by the cells, which suggests that the fluorescence in ACPP-DY676 treated cells is a result of activation and internalization. Our results also correspond to research reports, which show that almost all the cancer cell lines we studied [Roomi et al., 2009] and even the non-cancer cell line HMEC-1 [Taraboletti et al., 2002; Abecassis et al., 2003] express some level of MMPs 2 and 9. Interestingly, enzyme activity assay with the whole cells or more important with cell culture supernatant revealed results that partly correlate to the activation of ACPP and their uptake. In both cases the enzymatic activity measured for the HT-1080 cells were significantly higher ($P < 0.05$) than that detected in the HMEC-1, MDA-MB231, and BT-474 cells (supplementary data S2). But, we have to consider that cleavage of the ACPP-linker by other proteases may also activate them. Further controls with cell lines lacking MMP expression will be necessary to strengthen the evidence for MMP-based activation of the ACPP.

CONCLUSIONS

Near-infrared fluorescence allows highly sensitive measurements in cells, tissues, and organs without interference by fluorescent cell and tissue components. The CPPs in this investigation showed strong differences in transport efficiencies for fluorescent-labeled BSA and antibody into the human fibrosarcoma cell line HT-1080, resulting from different affinities to both cargos and therefore different abilities to form non-covalent complexes and from different uptake efficiencies of the formed complexes. Use of a protease activatable cell-penetrating peptide successfully transported the activated fluorescent fragment into cells expressing the MMPs 2 and 9, thus primarily labeling tumor cells. Our results show that the uptake is selective, but not as high as expected. To further improve the uptake-selectivity, coupling to specific dendrimers should be used. The advantages of NIR-fluorescent protein cargos and ACPPs will be demonstrated more clearly in animal experiments.

ACKNOWLEDGMENTS

We thank Ms. Maria Poetsch from the Leibniz Institute of Natural Product Research and Infection Biology (Hans Knoell Institute, Jena) and Dr. Georg Greiner from the Centrum of Molecular Biomedicine (Jena) for performing MALDI-TOF measurements.

We are grateful to Jena Bioscience GmbH for providing the cell-penetrating peptides, kits for fluorescence labeling, and for their generous funding. The work was funded in part by the Deutsche Forschungsgemeinschaft grant HI-698/10–1.

REFERENCES

Abecassis I, Olofsson B, Schmid M, Zalcman G, Karniguian A. 2003. RhoA induces MMP-9 expression at CD44 lamellipodial focal complexes and promotes HMEC-1 cell invasion. Experim Cell Res 291:363–376.

Andreev OA, Engelman DM, Reshetnyak YK. 2010a. PH-sensitive membrane peptides (pHLIPs) as a novel class of delivery agents. Mol Membrane Biol 27:341–352.

Andreev OA, Karabadzhak AG, Weerakkody D, Andreev GO, Engelman DM, Reshetnyak YK. 2010b. PH (low) insertion peptide (pHLIP) inserts across a lipid bilayer as a helix and exists by a different path. Proc Natl Acad Sci USA 107:4081–4086.

Aguilera TA, Olson ES, Timmers MM, Jiang T, Tsien RY. 2009. Systemic in vivo distribution of activatable cell penetrating peptides is superior to that of cell-penetrating peptides. Integrative Biol 1:371–381.

Chaloin L, Vidal P, Heitz A, van Mau N, Mery J, Divita G, Heitz F. 1997. Conformations of primary amphipathic carrier peptides in membrane mimicking environments. Biochemistry 36:11179–11187.

Colditz MJ, Jeffree RL. 2012. Aminolevulinic acid (ALA)-protoporphyrin IX fluorescence guided tumour resection. Part 1: Clinical, radiological and pathological studies. J Clinical Neurosci 19:1471–1474.

Cornelius JF, Slotty PJ, El Khatib M, Giannakis A, Senger B, Steiger HJ. 2014. Enhancing the effect of 5-aminolevulinic based photodynamic therapy in human meningioma cells. Photodiagnosis and Photodynam Ther 11:1–6.

Crombez L, Aldrian-Herrada G, Konate K, Nguyen QN, McMaster GK, Brasseur R, Heitz F, Divita G. 2009. A new potent secondary amphipathic cell-penetrating peptide for siRNA delivery into mammalian cells. Mol Therapy 17:95–103.

Dekiwadia CD, Lawrie AC, Fecondo JV. 2012. Peptide-mediated cell penetration and target delivery of gold nanoparticles into lysosomes. J Pept Sci 18:527–534.

De la Garza-Ramos R, Bydon M, Macki M, Huang J, Tamago RJ, Bydon A. 2014. Fluorescent techniques in spine surgery. Neurolog Res DOI: http://dx.doi.org/10.1179/1743132814Y

Deshayes S, Plenat T, Aldrian-Herrada G, Divita G, Le Grimellec C, Heitz F. 2004. Primary amphipathic cell penetrating peptides: Structural requirements and interactions with model membranes. Biochemistry 43:7698–7706.

Diao Y, Han W, Zhao H, Zhu S, Liu X, Feng X, Gu J, Yao C, Liu S, Sun C, Pan F. 2011. Designed synthetic analogs of the α-helical peptide temporin-La with improved antitumor efficacies via charge modification and incorporation of the integrin αvβ3 homing domain. J Pept Sci 18:476–486.

Ezzat K, Helmfors H, Tudoran O, Juks C, Lindberg S, Padari K, El-Andaloussi S, Pooga M, Langel Ü. 2012. Scavenger receptor-mediated uptake of cell-penetrating peptide nanocomplexes with oligonucleotides. FASEB J 26:1172–1180.

Hamann FM, Brehm R, Pauli J, Grabolle M, Wilhelm F, Kaiser WA, Fischer D, Resch-Genger U, Hilger I. 2011. Controlled modulation of serum protein binding and biodistribution of asymmetric cyanine dyes by variation of the number of sulfonate groups. Molecular Imaging 10:258–269.

Ignatovich IA, Dizhe EB, Pavlotskaya AV, Akifiev BN, Orlov BSV, Perevozchikov AP. 2003. Of the HIV-1 Tat protein are transferred to mammalian cells by endocytosis-mediated pathways. Complex of plasmid DNA with basic domain 278:47–57.

Kalafut D, Anderson TN, Chmielewski J. 2012. Mitochondrial targeting of cationic amphiphilic polyproline helix. Bioorg & Med Chem Lett 22: 561–563.

Keller AA, Mussbach F, Breitling R, Hemmerich P, Kappe K, Wittig B, Braun M, Schaefer B, Lorkowski S, Reissmann S. 2014. Transduction of proteins into Leishmania tarentolae by formation of non-covalent complexes with cell-penetrating peptides. J Cell Biochem 115:243–252.

Keller AA, Mussbach F, Breitling R, Hemmerich P, Schaefer B, Lorkowski S, Reissmann S. 2013. Relationships between cargo, cell penetrating peptides and cell type for uptake of non-covalent complexes into live cells. Pharmaceuticals 6:184–203.

Krämer A, Mentrup T, Kleizen B, Rivera-Milla E, Reichenbach D, Enzensperger C, Nohl R, Täuscher E, Görls H, Ploubidou A, Englert C, Werz O, Arndt H-D, Kaether C. 2013. Small molecules intercept notch signaling and the early secretory pathway. Nature Chem Biol 9:731–740.

Kurzawa L, Pellerano M, Morris MC. 2010. PEP and CADY-mediated delivery of fluorescent peptides and proteins into living cells. Biochim Biophys Acta 1798:2274–2285.

Letoha T, Keller-Pinter A, Kusz E, Koloszi C, Bozso Z, Toth G, Vizier C, Olah Z, Szilak L. 2010. Cell-penetrating peptide exploited syndecans. Biochim Biophys Acta (Biomembranes) 1798:2258–2263.

Murphy G, Nagase H. 2008. Review: Progress in matrix metalloproteinase research. Molecular Aspects of Medicine 29:290–308.

Musial-Siwek M, Karabadzhak AG, Andreev OA, Reshetnyak YK, Engelman DM. 2010. Tuning the insertion properties of pHLIP. Biochim Biophys Acta 1798:1041–1046.

Mussbach F, Martin F, Zoch A, Schaefer B, Reissmann S. 2011. Tranduction of peptides and proteins into live cells by cell penetrating peptides. J Cell Biochem 112:3824–3833.

Nguyen QT, Olson ES, Aguilera TA, Jiang T, Scadeng M, Ellies LG, Tsien RY. 2010. Surgery with molecular fluorescence imaging using activatable cell-penetrating peptides decreases residual cancer and improves survival. Proc Natl Acad Sci USA 107:4317–4322.

Olson ES, Aguilera TA, Jiang T, Ellies LG, Nguyen QT, Wong EH, Gross LA, Tsien RY. 2009. In vivo characterization of activatable cell-penetrating peptides for targeting protease activity in cancer. Integrative Biology 1:382–393.

Olson ES, Tao J, Aguilera TA, Nguyen QT, Ellies LG, Scadeng M, Tsien RY. 2010. Activatable cell penetrating peptides linked to nanoparticles as dual probes for in vivo fluorescence and MR imaging of proteases. Proc Natl Acad Sci USA 107:4311–4316.

Olson ES, Whitney MA, Friedman B, Aguilera TA, Crisp JL, Baik FM, Jiang T, Baird SM, Tsimikas S, Tsien RY, Nguyen QT. 2012. In vivo fluorescence imaging of atherosclerotic plaques with activatable cell-penetrating peptides targeting thrombin activity. Integrative Biology 4:595–605.

Puppa AD, Rustemi O, Gioffre G, Troncon I, Lombardi G, Rolma G, Sergi M, Munari M, Cecchin D, Gardiman MP, Scienza R. 2014. Predictive value of intraoperative 5-aminolevulinic acid-induced fluorescence for detecting bone invasion in meningioma surgery. J Neurosurg 120:840–845.

Radis-Baptista G, de la Torre BG, Andreu D. 2008. A novel cell-penetrating peptide sequence derived by structural minimization of a snake toxin exhibits preferential nucleolar localization. J Med Chem 51:7041–7044.

Reshetnyak YK, Andreev OA, Segala M, Markin VS, Engelman DM. 2008. Energetics of peptide (pHLIP) binding to and folding across a lipid bilayer membrane. Proc Natl Acad Sci USA 105:15340–15345.

Roomi MW, Monterrey JC, Kalinovsky T, Rath M, Niedzwiecki A. 2009. Patterns of MMP-2 and MMP-9 expression in human cancer cell lines. Oncology Rep 21:1323–1333.

Savanier EN, Felsen CN, Nashi N, Jiang T, Ellies LG, Steinbach P, Tsien RY, Nguen QuT. 2013. Real-time in vivo molecular detection of primary tumors and metastases with ratiometric activatable cell-penetrating peptides. Cancer Research 73:855–864.

Sbardella D, Fasciglione GF, Gioia M, Ciaccio M, Tundo GR, Marini S, Coletta M. 2012. Review: Human matrix metalloproteinases: An ubiquitarian class of enzymes involved in several pathological processes. Molecular Aspects of Medicine 33:119–208.

Shu X, Royant A, Lin MZ, Aguilera TA, Lev-Ram V, Steinbach PA, Tsien RY. 2009. Mammalian expression of infrared fluorescent proteins engineered from a bacterial phytochrome. Science 324:804–807.

Snyder EL, Saenz CC, Denicourt C, Meade BR, Cui X-S, Kaplan IM, Dowdy SF. 2005. Enhanced targeting and killing of tumor cells expressing the CXC chemokine receptor 4 by transducible anticancer peptides. Cancer Res 65:10646–10650.

Szeto HH, Schiller PW, Zhao K, Luo G. 2005. Fluorescent dyes alter intracellular targeting and function of cell-penetrating peptides. FASEB J 19:118–120.

Taraboletti G, D'Ascenzo, Borsotti P, Giavazzi R, Pavan A, Dolo V. 2002. Shedding of the matrix metalloproteinases MMP-2, MMP-9, and MT1-MMP as membrane vesicle-associated compomemts by endothelial cells. Amer J Pathol 160:673–680.

Torchilin VP. 2008. Tat peptide-mediated intracellular delivery of pharmaceutical nanocarriers. Advanced Drug Deliv Rev 60:548–558.

van Duijnhoven SMJ, Robillard MS, Nicolay K, Gruell H. 2011. Tumor-targeting of MMP-2/9 activatable cell-penetrating probes is caused by tumor-independend activation. J Nuclear Med 52:279–286.

Vives E, Brodin P, Lebleu B. 1997. A truncated HIV-1 Tat protein basic domain rapidly translocates through the plasma membrane and accumulates in the cell nucleus. J Biol Chem 272:16010–16017.

Whitney M, Savariar EN, Friedman B, Levin RA, Crisp JL, Glasgow HL, Lefkowitz R, Adams SR, Steinbach P, Nashi N. 2013. Ratiometric activatable cell-penetrating peptides provide rapid in vivo readout of thrombin activation. Angewandte Chemie 52:325–330.

Yousif LF, Stewart KM, Horton KL, Kelley SO. 2009. Mitochondria-penetrating peptides: Sequence effects and model cargo transport. ChemBioChem 10:2081–2088.

SUPPORTING INFORMATION

Additional supporting information may be found in the online version of this article at the publisher's web-site.